

# LIDAR ACQUISITION and CONTROL SURVEY REPORT

Subcontract Agreement: S/C-USGS-G10PC00013-17  
Task order: G10PD2249 – Salton Sea Lidar

*Prepared for*



*Prepared by*



**TOWILL** | Surveying, Mapping  
and GIS Services

November, 2010

---

## EXECUTIVE SUMMARY

Under contract with Dewberry and Davis (Dewberry), Towill acquired high resolution Lidar data (nominal point spacing of 0.5 meters) within a 5-mile buffer ring of the shoreline of the Salton Sea located in Southern California. The data were acquired in 9 missions over the course of 5 days in November, 2010.

As part of the campaign, a 3-dimensional primary survey network consisting of local Continuous GPS (CGPS) stations and a semi-permanent base station point was observed to establish the basis of control for the Lidar data. The selected horizontal and vertical datums upon which the Lidar data are processed are NAD83(CORS); epoch of 2010.73 and the North American Vertical Datum of 1988 (NAVD88) as realized by the reported coordinates and ellipsoid heights of the common CGPS stations shared with the McGee Survey, contracted by Dewberry, and the application of GEOID09. This primary network satisfied U.S. Federal Geodetic Control Subcommittee (FGCS) standards for Order B geodetic GPS surveys (8mm + 1 part per million).

In addition, 40 check points and 5 existing NGS bench marks were surveyed to demonstrate the absolute accuracy of the Lidar data. The root-meant-square (RMS) of the differences between the check point surveyed elevations and the Lidar-derived surface model was 0.036 meters.

Rigorous Lidar sensor calibration and quality control procedures were applied during the course of the campaign. Calibration passes were flown at the beginning and end of each mission and analyzed to verify the performance of the sensor and to make small adjustments to the final processing parameters.

In summary, all of the project's geodetic surveying and mapping goals were achieved. This report provides detailed documentation of all aspects of the work.

**Towill, Inc.**



Keith Kirkby  
*Geodetic Engineer*  
November, 2010

## TABLE OF CONTENTS

<b>1.</b>	<b>INTRODUCTION .....</b>	<b>1</b>
	1.1 Points of Contact .....	1
<b>2.</b>	<b>CONTROL SURVEY AND DATUMS .....</b>	<b>2</b>
	2.1 Introduction .....	2
	2.2 Project Survey Datums .....	2
	2.3 Field Equipment and Procedures .....	2
	2.4 Primary Survey Network and Adjustment .....	3
<b>3.</b>	<b>LIDAR DATA ACQUISITION AND PROCESSING .....</b>	<b>6</b>
	3.1 Introduction .....	6
	3.2 Data Acquisition .....	6
	3.3 Airborne GPS Processing .....	6
	3.4 IMU Processing and Best Estimated Trajectory .....	8
	3.5 Lidar Point Cloud Processing .....	8
<b>4.</b>	<b>LIDAR CALIBRATION AND QC .....</b>	<b>10</b>
	4.1 Introduction .....	10
	4.2 Calibration Overflights .....	10
	4.3 Additional Calibration .....	11
<b>5.</b>	<b>LIDAR CHECKPOINT QA .....</b>	<b>13</b>

## LIST OF TABLES

TABLE 1.	ABSOLUTE LOOP MISCLOSURES .....	5
TABLE 2.	PRIMARY NETWORK ADJUSTMENT WEIGHTED CONSTRAINTS .....	5
TABLE 3.	KINEMATIC QA ROUTE STATISTICS .....	13
TABLE 4.	LIDAR CHECK POINT RESIDUALS .....	14

---

## TABLE OF CONTENTS (CONT.)

### LIST OF FIGURES

FIGURE 1. PRIMARY SURVEY NETWORK DIAGRAM.....	4
FIGURE 2. LIDAR DATA AND PROCESS FLOW .....	7
FIGURE 3. GENERAL PROJECT LIDAR ACQUISITION PARAMETERS .....	8
FIGURE 4. POST-PROCESSED GRAFNAV SOLUTION - LIFT 314A.....	9
FIGURE 5. FORWARD VS. REVERSE POST-PROCESSED SOLUTION - LIFT 314B.....	9
FIGURE 6. EXAMPLE OF A CALIBRATION OVERFLIGHT.....	10
FIGURE 7. MISSION-BY-MISSION CALIBRATION PASS ANALYSES .....	12

### APPENDICES

APPENDIX I. FINAL COORDINATES AND ELEVATIONS.....	15
APPENDIX II. FULLY CONSTRAINED NETWORK ADJUSTMENT .....	20

## **1. INTRODUCTION**

This document provides a comprehensive overview of the Lidar acquisition campaign to acquire high-density Lidar data within a 5-mile wide shoreline ring around the Salton Sea located in Southern California. The report describes the field survey associated with establishing base stations to support the airborne GPS (AGPS) component of the campaign, Lidar system calibration, Lidar data post-processing, and QA/QC of the data.

The Lidar acquisition was completed in a total of 9 separate flight missions between November 9th and November 13th inclusive. Flight operations were staged out of the Jackie Cochrane Regional Airport located in Thermal, California.

All data acquisition field work, data post-processing and quality analysis was completed by Towill personnel. The components of the campaign include:

- Establishing and surveying AGPS base stations, control, and check points;
- Verifying Lidar system calibration and post-processing parameters;
- Airborne GPS (AGPS) and IMU data post-processing;
- Pre and post-mission control surface overflight data analysis;
- Surface check point survey analysis;

### **1.1 Points of Contact**

Please direct any questions regarding the contents of this document to:

**Becky Morton**  
Project Manager  
Towill, Inc.  
Phone: (415) 243-4384 x.130  
Fax: (415) 243-8264  
Mobile: (916) 212-8206  
becky.morton@towill.com

**Keith Kirkby**  
Geodetic Engineer  
Towill, Inc.  
Phone: (719) 355-1150 x.403  
Fax: (719) 355-1155  
Mobile: (719) 243-5990  
keith.kirkby@towill.com

---

## **2. Control Survey and Datums**

### **2.1 Introduction**

Dewberry and Davis contracted McGee Surveying Consulting to perform a detailed geodetic survey in the vicinity of the project area to analyze the local vertical control and establish independent Lidar check data. The survey incorporated several existing NGS benchmarks and CGPS (Continuous GPS) stations scattered throughout the project area. As a result of the McGee survey and subsequent analysis, it was determined that the underlying control for this project will be based on the published orthometric elevation of a single benchmark located on the east side of the project area (DHLGA, PID: AH8516). The horizontal control for the project is based on the published coordinates of the local CGPS sites in the area in the mid-epoch of survey (2010.73).

Towill observed a primary geodetic network consisting of CGPS stations and a base station point established at the airport of operations to support the airborne GPS component of the Lidar campaign thereby ensuring a consistent horizontal and vertical datum realization across the entire extent of the project area as realized by the McGee survey (see Figure 1). The network consists of 10 CGPS and 1 designated GPS base station.

Independent CGPS observation data were downloaded in the days leading up to the start of the acquisition campaign to establish the relative baseline observations between the CGPS stations. The remaining baselines were observed using the data from the base station occupations during acquisition and additional CGPS data from those respective days.

Final coordinates and elevations of the base station locations were established via a 3-dimensional network adjustment constrained to the published horizontal coordinates and ellipsoid heights of the CGPS (as described in section 2.5, below).

In addition, 40 check points and 5 existing NGS bench marks (shared with the McGee survey) were surveyed during the Lidar acquisition. These locations were surveyed with respect to the operating base stations and nearby CGPS stations.

### **2.2 Project Survey Datums**

The horizontal datum for this project is NAD83(CORS), epoch of 2010.73, the mid-epoch of the McGee survey. The datum is realized by the horizontal coordinates reported from the McGee Survey of several CGPS stations (see Table 2).

The vertical datum for this project is NAVD88. The datum is realized by the ellipsoid heights of the same CGPS station reported from the McGee Survey and the application of the geoid model GEOID09.

### **2.3 Field Equipment and Procedures**

All GPS observations were accomplished using Trimble Navigation R7 dual frequency GPS receivers and accompanying Trimble Zephyr Geodetic antennae. Relative static surveying techniques were used for all baseline observations. Instrument heights were measured twice in units of feet and meters and the values reduced and compared in the field prior to leaving each station.

In general, base station data were logged for the duration of the acquisition on any given day (typically 4 to 12 hours) and check point data were logged for a minimum of 30 minutes and as much as 90 minutes depending on proximity to operating base stations and/or CGPS station.

---

## 2.4 Primary Survey Network and Adjustment

Observed relative GPS baselines were processed in Trimble Business Center. All processed observations consist of quasi-independent baselines (i.e. in accordance with the “ $n-1$  baselines” rule where  $n$  = number of receivers in a given ‘session’). The International GPS Service for Geodynamics (IGS) rapid precise orbits (igr) were used in the processing of all baseline vectors. The ‘igr’ orbits are published with a latency of approximately 30 hours. These orbits are globally accurate to within ~5cm and are particularly important when processing long baselines.

The absolute horizontal and vertical GPS loop misclosures for the primary network are presented in Table 1. The spatial misclosures in parts per million (ppm) are also listed. All loops comprise quasi-independent baselines from at least two ‘sessions’.

The primary survey network, consisting of 11 points and 19 baselines, was designed to provide a basis for the Lidar control (i.e. AGPS base stations) and establishing additional quality control points for this project. A minimally constrained adjustment was executed to verify the internal integrity of the network, establish *a priori* weights for the GPS observations, and judge the absolute fit of the constraints.

The GPS baselines vector components were adjusted using Microsearch™ GEOLAB 2001 (version 2001.9.20.0). *A priori* weights for the observations were based on the scaled variance–covariance sub-matrices estimated by the Trimble Business Center software. In the resulting adjustment, the estimated variance factor ( $\hat{\sigma}_o^2 = 1.0765$ ) passed the  $\chi^2$ -test indicating appropriate *a priori* estimates of the accuracy of the GPS baseline vectors. None of the 57 vector component residuals or associated standardized residuals were flagged for possible rejection under the  $\tau$ -max test at the 95 percent level of confidence. The relative horizontal accuracy of the network can be assessed by reviewing the relative 95 percent confidence regions (ellipses) of the adjustment. All station pairings meet the Federal Geodetic Control Subcommittee (FGCS) relative positioning standard for Order B surveys (8mm + 1ppm).

In a second, fully constrained adjustment, the NAD83 latitude, longitude and ellipsoid height of the 7 CGPS stations shared with the McGee Survey were held as *weighted* constraints (see Table 2). The estimated variance factor ( $\hat{\sigma}_o^2 = 1.0286$ ) indicates that the network is not being unduly distorted by the imposition of the constraints and is maintaining its internal integrity. The adjustment yields coordinates on the NAD83(CORS), epoch 2010.73 and orthometric elevations relative to NAVD88 via the GEOID09 geoidal model. These coordinates serve as the control for the post-processing of all Lidar data and subsequent products derived from the Lidar data. See Appendix II for the primary constrained adjustment listing.

A third and final adjustment was run to incorporate the check point and bench mark observations. The adjusted coordinate values from the fully constrained adjustment were held as *fixed* constraints to derive final coordinate and elevation values of the check points. Appendix I tabulates the final adjusted coordinate and elevation values of all surveyed points.

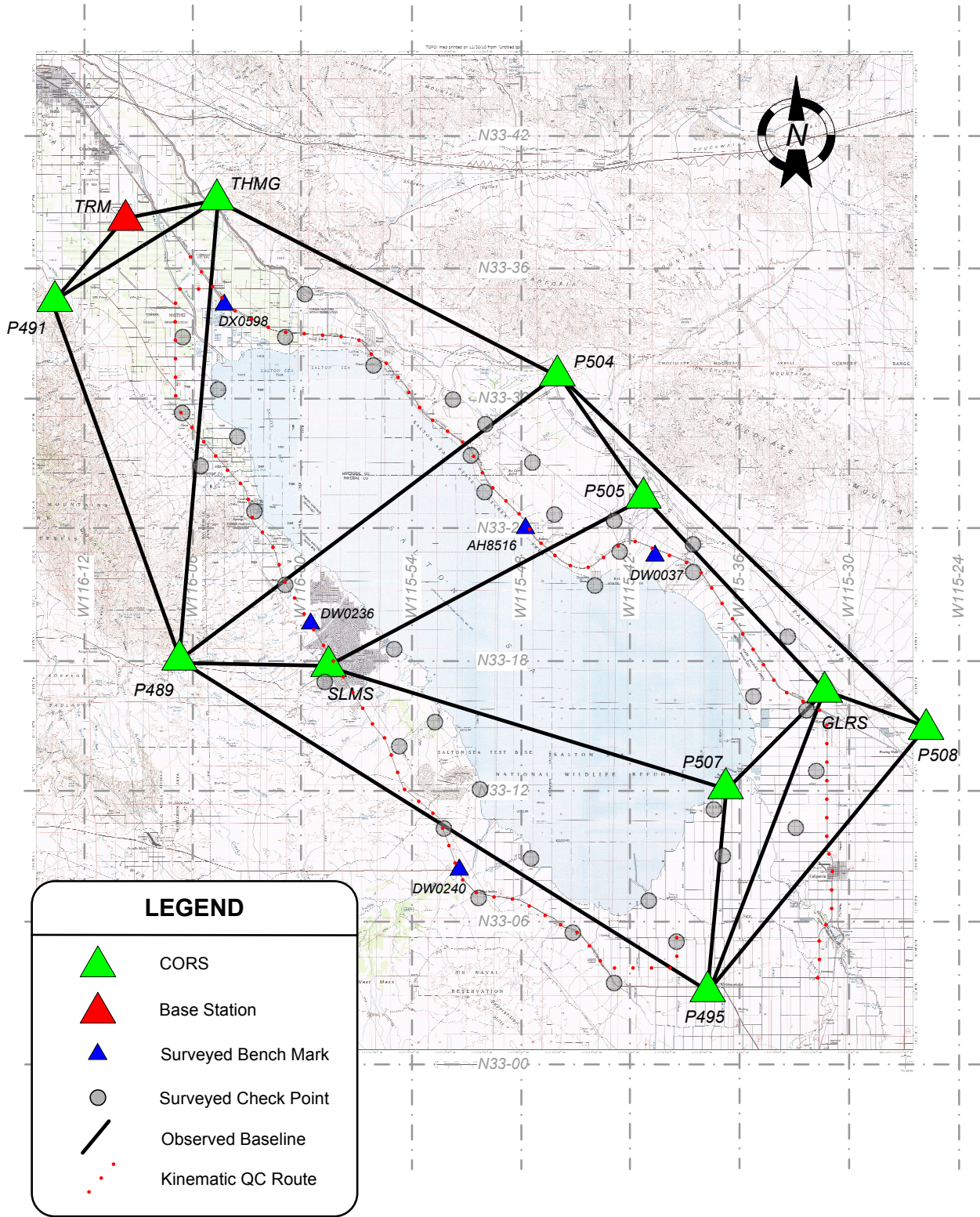


Figure 1. Primary Survey Network Diagram



Table 1.  
 Absolute Loop Misclosures

Loop	Horizontal Misclosure [mm]	Vertical Misclosure [mm]	Loop Length [meters]	PPM
TRM - THMG - P491 - TRM	5	2	33366	0.16
P491 - THMG - P489 - P491	2	1	88372	0.03
THMG - P504 - P489 - THMG	5	4	112346	0.06
P489 - P504 - P505 - SLMS - P489	6	4	96227	0.07
SLMS - P505 - GLRS - P507 - SLMS	3	3	100790	0.04
P489 - SLMS - P507 - P495 - P489	5	8	118279	0.08
P504 - P508 - GLRS - P505 - P504	11	4	87623	0.14
P507 - GLRS - P495 - P507	5	2	56503	0.10
GLRS - P508 - P495 - GLRS	4	0	65725	0.07

Table 2.  
 Primary Network Adjustment Weighted Constraints

Horizontal Datum: NAD83(CORS)  
 Epoch: 20010.73  
 Linear Unit: International Meter

Point	Source	Latitude				Longitude				Ellipsoid Height	Adjustment Residuals (m)		
		°	'	''	U.S. Feet	°	'	''	U.S. Feet		Lat.	Lng.	Hgt.
GLRS	McGee	N	33	16	29.31042	W	115	31	16.89020	-47.867	-0.002	-0.002	0.002
P491	McGee	N	33	34	28.83021	W	116	13	36.51934	5.023	0.004	0.005	-0.001
P504	McGee	N	33	30	59.06379	W	115	45	57.00099	84.804	-0.002	0.000	-0.007
P505	McGee	N	33	25	25.93184	W	115	41	13.14995	-57.019	0.001	-0.005	0.005
P507	McGee	N	33	11	59.90190	W	115	36	44.60941	-77.652	0.000	0.000	0.006
SLMS	McGee	N	33	17	32.00638	W	115	58	40.18320	-45.158	0.003	0.001	0.005
THMG	McGee	N	33	39	02.29054	W	116	04	38.05130	34.417	-0.003	0.001	-0.011

Notes: Ellipsoid heights are to the Antenna Reference Point (ARP) of the CGPS

---

### 3. LIDAR DATA ACQUISITION AND PROCESSING

#### 3.1 Introduction

Following is an overview description of the procedures applied in this Lidar campaign from acquisition to final processed data. Figure 2 illustrates the general flow of the data through the multiple processes required to generate the Lidar point cloud in the 'LAS' version 1.2 format.

#### 3.2 Data Acquisition

The Lidar data acquisition was completed within 9 lifts, or missions. All missions originated and/or terminated at the Jackie Cochrane Regional Airport. A GPS base station was operating at the airport during every lift. UNAVCO, the administrating entity of the Plate Boundary Observatory which consists of dozens of CGPS stations located throughout the western states, was contacted prior to the start of the Lidar acquisition to arrange for 1 Hertz data logging of several of the CGPS stations included in the primary survey network. The data from these stations were downloaded and applied in the post-processing of the kinematic AGPS data.

The target flying height for this project was 800 meters above mean terrain (AMT). This target height was unattainable over an area of heavy relief located in the northwest corner of the project. The voids created by the reduction in coverage associated with the reduced flying height over this terrain were filled in with additional flight lines. The "fill-in" lines were acquired with a lower pulse rate setting (100kHz versus 150kHz) to prevent a "multi-pulse" situation from occurring near the beginning or end of each fill-in line where the ground was at the lower elevation. Desired point density was achieved by virtue of the lower flying height despite the reduction in pulse rate.

Figure 3 summarizes the general acquisition parameters applied project-wide (with the exception of the 9 short fill-in lines over the high terrain located to the northwest of the project area).

Kinematic GPS and Inertial Measurement Unit (IMU) data were acquired by the Applanix POS Inertial Navigation System during the missions. The post-processed POS data results in a 200 Hertz, 6-parameter aircraft trajectory (x, y, z, roll, pitch, yaw).

The Airborne GPS (AGPS) and IMU data were processed immediately following each mission. In addition, a sample of the Lidar data was post-processed at the completion of the missions and the data was reviewed to ensure correct system operation and data coverage.

#### 3.3 Airborne GPS Processing

The quality of the Airborne GPS data represents a significant component of the overall error budget with respect to the accuracy of the Lidar data. It is important to exercise vigilance in the validation of the integrity of the AGPS solution. This effort begins prior to acquisition with careful mission planning to identify periods of the day during which satellite availability and/or geometry may not be conducive to an acceptable solution. Data acquisition is generally scheduled around these periods (other constraints such as airspace restrictions, daylight conditions and weather notwithstanding).

The kinematic AGPS data was post-processed using Novatel, Inc.'s Grafnav version 8.20 software, the *de facto* kinematic GPS post-processing package in the airborne remote sensing industry. Data is post-processed forward and backward in time exploiting the software's robust Kinematic Ambiguity Resolution and Multi-Baseline features to mitigate ambiguity drift and minimize poor data as a result of satellite loss of lock (see example in Figure 4). Figure 5 illustrates the comparison of the forward and reverse solutions of the post-processed GPS data for one of the missions. The plot exhibits a very satisfactory solution and it represents the standard results achieved in the post-processing of all missions.

### LIDAR Data Post-Processing Data Flow

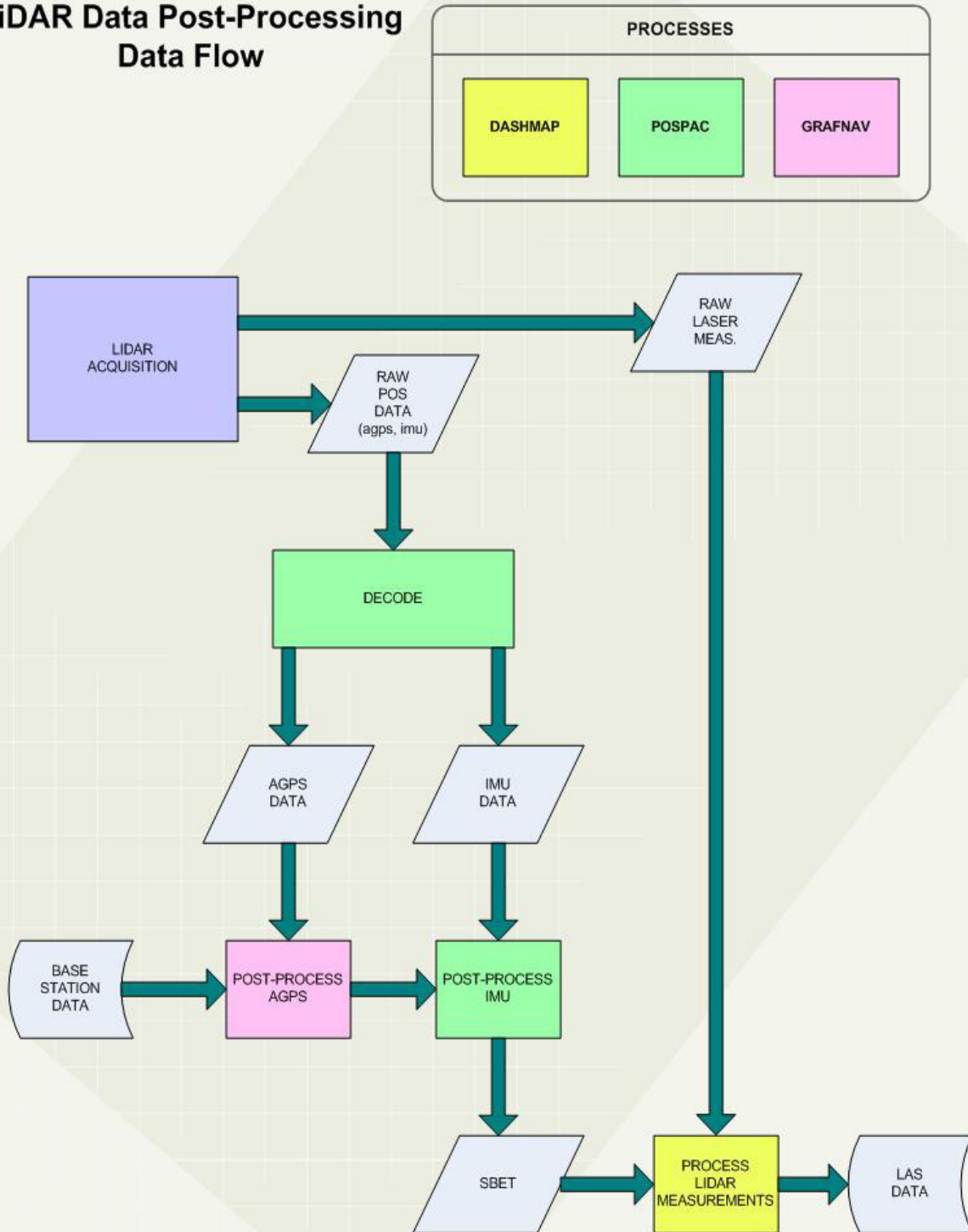


Figure 2. Lidar Data and Post-Processing Data Flow

Flight Profile		LIDAR Settings	
Altitude (m AGL)	800	System PRF (kHz)	150
Unaided NOHD (m)	122	Scan Freq (Hz)	62
Pass Heading (deg)	320	Scan Angle +/-	16
Overlap (%)	30	Scan Offset	0
Speed (kts)	120	Desired Res (m)	0.434
Turn Time (min)	5	Cross Track Res	0.379
Passes	43	Down Track Res	0.498
Pass Spacing (m)	320.73	PPM^2	5.3
Min DEM Altitude	0	Scan Cutoff (deg)	0.02
		Swath (m)	458.19

Figure 3. General Project Lidar Acquisition Parameters

### 3.4 IMU Processing and Best Estimated Trajectory

The post-processed AGPS trajectory is combined with the raw 200 Hertz IMU observations in a loosely-coupled Kalman filter-based processing algorithm to produce the final high-frequency Smoothed Best Estimated Trajectory (SBET). Applanix's POSPac software, version 4.4, is employed in this process.

Given a good quality AGPS solution and clean, gap-free IMU data, this process generally runs very smoothly. The field procedure includes several minutes of static GPS and IMU data collection prior to departure to allow sufficient time for the IMU to acquire a fine local level. The data is acquired in duplicate in real-time to ensure a high-quality record set. The IMU processing was clean and consistent for all missions during this campaign.

The final, high-frequency SBET is the source of absolute geo-referencing of the post-processed Lidar point cloud. The SBET is introduced into the final phase of the Lidar data processing.

### 3.5 LIDAR Point Cloud Processing

Final Lidar data processing is accomplished using Optech's DASHMap software, version 5.01. The decoded raw laser observations (ranges, intensities, and mirror angles) and the final processed SBET are combined within DASHMap to compute the final 3-dimensional coordinates of the return(s) of each laser pulse.

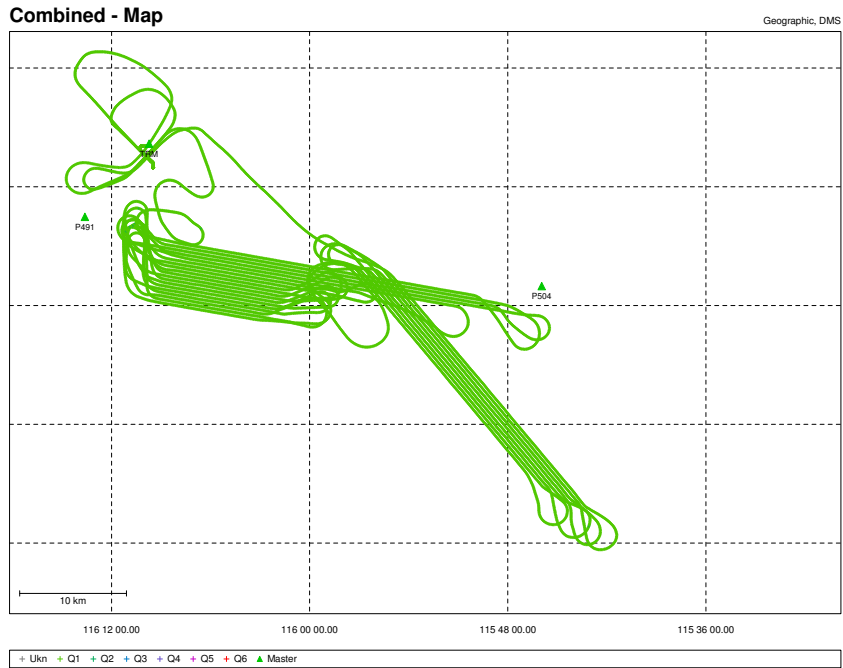
Based on the daily calibration analysis, described in the following section of this report, several of the Lidar parameters are slightly adjusted within DASHMap on a mission-by-mission basis.

The calibrated data is output in LAS format, version 1.2 with "adjusted" GPS times (defined as GPS seconds of the week minus  $1 \times 10^{-9}$  seconds).



Project: Day314A

GrafNav v8.20.0522



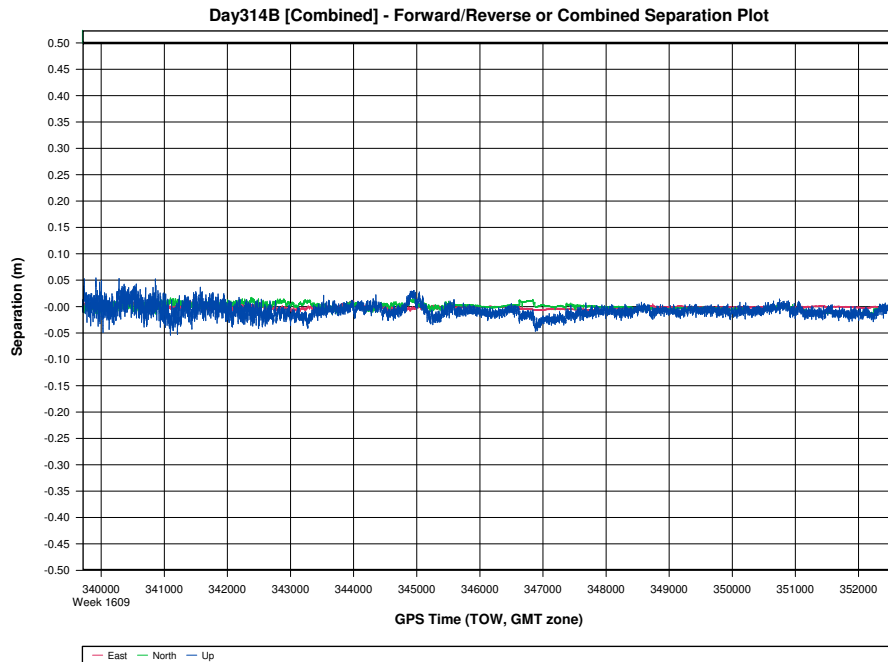
11/30/2010

Page 1

Figure 4. Post-Processed GrafNAV Solution - Lift 314A

Project: Day314B

GrafNav v8.20.0522



11/30/2010

Page 1

Figure 5. Forward vs. Reverse Post-Processed Solution - Lift 314B

## 4. LIDAR CALIBRATION AND QC

### 4.1 Introduction

The Optech Orion M200 Lidar system is subject to a regular maintenance and calibration schedule. The intent of periodic calibration is to monitor and validate components of the overall error budget including IMU boresight and performance, mirror angle readings and pulse gate timing. Several of these parameters can vary during and between missions due to changes in ambient meteorological conditions, different flying heights above ground, and different acquisition variables. As such, regular checks on the calibration were carried out during every mission.

### 4.2 Calibration Overflights

To assure that the LIDAR system is performing within specifications, on a mission-by-mission basis, a snapshot of data is captured over a known surface, most often one of the runways located at the airport of operations. The runway surface is surveyed by collecting hundreds of topographic points using a post-processed kinematic GPS procedure.

At the beginning and end of each mission, two passes are made in opposite directions at right angles to and over the surveyed runway (see Figure 6, below). On average, approximately 80,000 Lidar points are acquired over the runway surface per pass. The surveyed topographic points that define the “known” surface of the runway are used to develop a surface model and the Lidar points from each pass are draped over this model and residuals computed. The residuals from each pass are graphed versus distance along the runway to provide an effective vertical cross-section of the entire Lidar swath at a short moment in time.

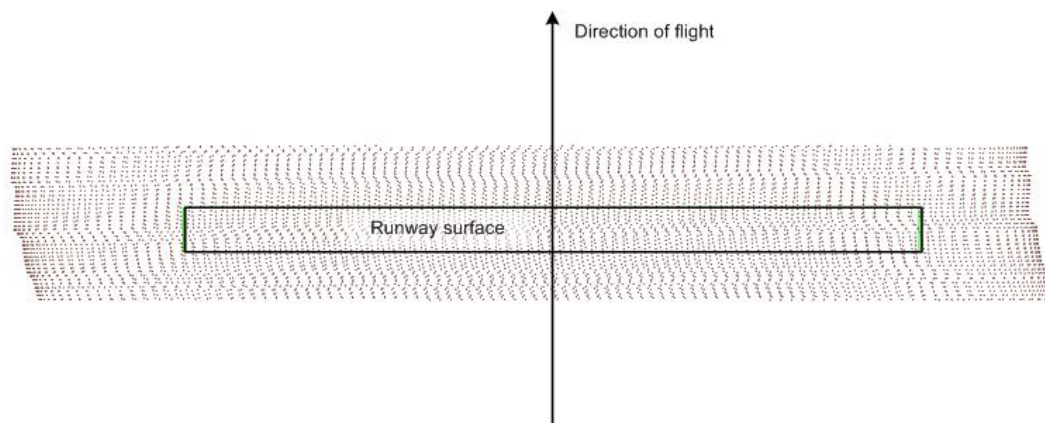


**Figure 6. Example of a Calibration Overflight**

The graphs from each pass are used to check that the mirror angle offset and scale, IMU solution roll and pitch bias, and elevation bias are within acceptable tolerances and to finely tune the general parameters on a mission-by-mission basis. This “snapshot” of the Lidar swath also ensures that the system is operating normally and that there are no anomalies contained in the data.

Figure 7 contains a plot of an unbiased runway overflight computed for each mission during the campaign. The following information may be obtained through careful examination of the graphs:

- The 99-percent noise band of the data is consistent at approximately 10 centimeters or less;
- There is no significant mirror scale error (characterized by a smile or frown);

- 
- There is no significant roll error (characterized by a tilt in the noise band);
  - There are no evident data anomalies;

Each plot is accompanied by the average residual and root mean square (RMS) of the residuals for the respective data set. Of the 9 data sets, the largest RMS is 6.4 centimeters, a representation of the combined stochastic noise and bias of the Lidar data prior to any vertical adjustment. The plots and statistics demonstrate that the system is working well within the system specifications.

### 4.3 Additional Calibration

The runway passes also serve to examine potential pitch and yaw biases that may be present in the data. These parameters are typically more stable over the course of the campaign and are therefore checked only periodically during the acquisition period.

The pitch bias can be analyzed by examining data flown in opposite directions over an area with a sharp change in elevation, such as the edge of a building perpendicular to the direction of flight. A pitch bias will manifest itself as a “ghosting” of the edge of the building by virtue of the opposite direction passes.

In a similar fashion, a bias about the normal axis (yaw) can be detected simply by observing the intensity return images from orthogonal flight lines of obvious features such as the runway center line. A yaw bias will cause a difference in orientation yielding an obvious displacement of visible features.

The results of these various calibration and QC analyses are applied in the mission-by-mission processing of the data to ensure a consistent and accurate overall data set.

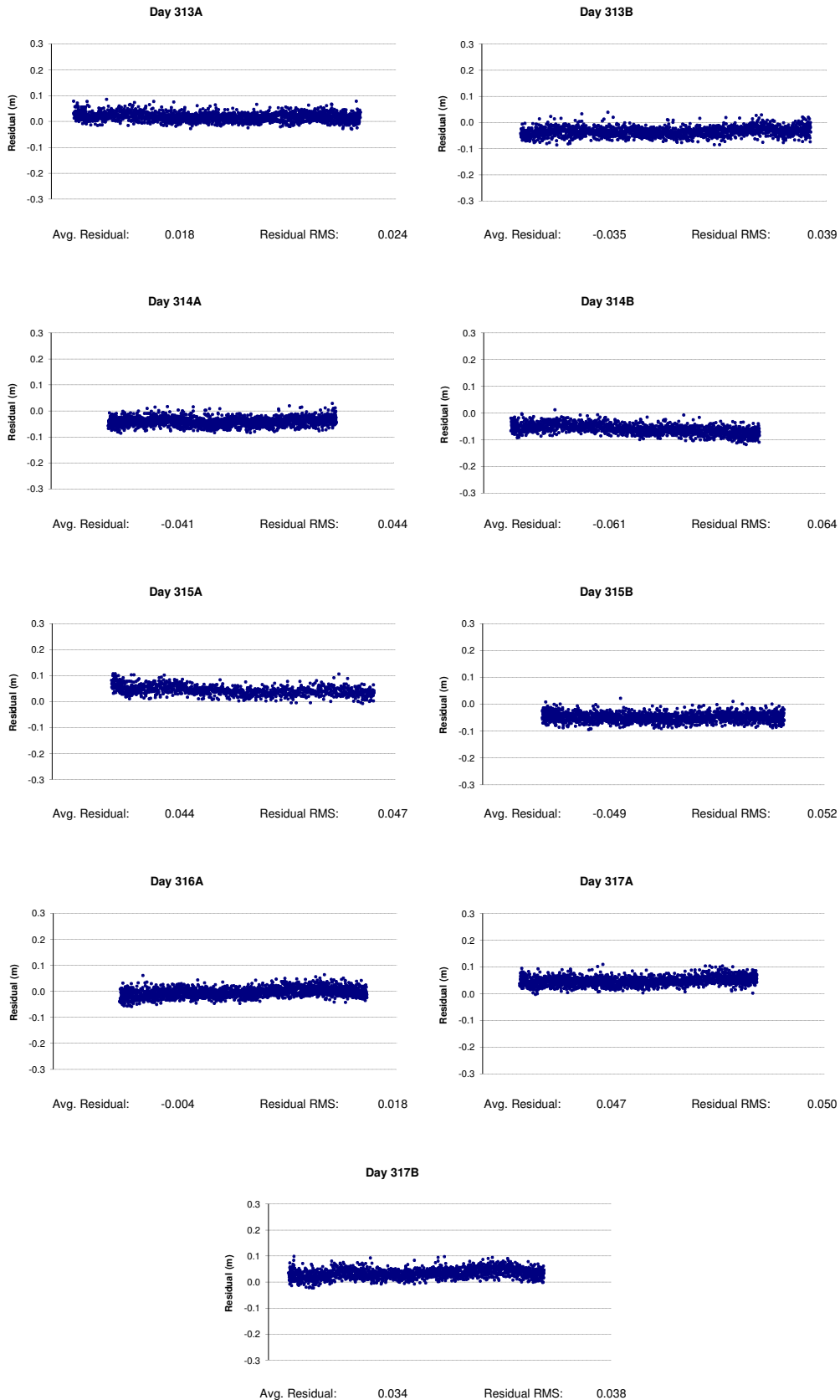


Figure 7. Mission-by-Mission Calibration Pass Analyses



## 5. LIDAR CHECKPOINT QUALITY ASSURANCE

In a further effort to validate the absolute vertical accuracy of the Lidar-derived elevations, 40 well-distributed check points were established and surveyed with respect to the AGPS base stations and CGPS stations that were included in the primary survey network.

In the vicinity of each check point, the post-processed Lidar data is used to generate a surface model upon which the check point is draped. The residual elevation difference is computed at each check point location. Table 4 summarizes the results of the check point analysis in meters. The NGS benchmarks that were incorporated into the McGee survey (a subset of which were included in the Towill Survey) were also included in this analysis, where practicable (i.e. benchmarks located on suitable ground surfaces). The RMS of all check point differences is 0.036 meters.

Additionally, two kinematic GPS routes were established along both the west and east sides of the project area (see Figure 1). This was accomplished by mounting a GPS antenna on the roof of a vehicle and driving along the respective primary highways at normal highway speeds. The kinematic data was post-processed using the same CGPS stations that were used to support the Lidar data reductions.

Data from the kinematic QA post-processing was output at a 10-second interval and checked against the Lidar data in the same manner as the static QA points. This process is designed primarily as a gross check on the consistency of the Lidar data since the offset between the antenna location and the ground is highly variable with changing speeds and vehicle loads.

Several points were either automatically or manually removed from the analysis due to obstructions (primarily trucks and other vehicles) located within the Lidar data. Any point that was manually removed was visually checked against the Lidar data to verify the presence of an obstruction. The occurrence of vehicles located within the Lidar data was much more prevalent on the west route, a major north-south highway in the valley.

The statistical results of each pass are reported in Table 3, below.

Table 3. Kinematic QA Route Statistics

<b>Kinematic Route - West</b>	
Total Samples	310
Samples Outside of Lidar Coverage	3
Samples Removed Due To Obstruction	37
<b>Minimum</b>	<b>-0.074</b>
<b>Maximum</b>	<b>0.097</b>
<b>Average</b>	<b>0.018</b>
<b>Standard Deviation</b>	<b>0.032</b>
<b>RMS</b>	<b>0.037</b>

<b>Kinematic Route - East</b>	
Total Samples	253
Samples Outside of Lidar Coverage	5
Samples Removed Due To Obstruction	2
<b>Minimum</b>	<b>-0.078</b>
<b>Maximum</b>	<b>0.068</b>
<b>Average</b>	<b>-0.007</b>
<b>Standard Deviation</b>	<b>0.027</b>
<b>RMS</b>	<b>0.029</b>



Table 4.

**LIDAR CHECK POINT RESIDUALS**  
Ellipsoid Heights (International Meter)

Point	Surveyed Elev.	LIDAR Elev.	Residual
1	-93.212	-93.260	-0.048
2	-89.147	-89.110	0.037
3	-11.306	-11.280	0.026
4	-101.778	-101.780	-0.002
5	-28.309	-28.340	-0.031
6	-96.612	-96.600	0.012
7	-75.114	-75.160	-0.046
8	-101.964	-101.980	-0.016
9	-66.935	-66.990	-0.055
10	-42.754	-42.760	-0.006
11	-83.213	-83.220	-0.007
12	-94.810	-94.810	0.000
13	-100.785	-100.780	0.005
14	-49.798	-49.820	-0.022
15	-88.366	-88.370	-0.004
16	-52.241	-52.270	-0.029
17	-99.213	-99.180	0.033
18	-82.998	-83.030	-0.032
19	-90.570	-90.560	0.010
20	-95.693	-95.680	0.013
21	-104.042	-104.110	-0.068
22	-98.113	-98.100	0.013
23	-92.742	-92.720	0.022
24	-102.579	-102.600	-0.021
25	-81.788	-81.730	0.058
26	-83.229	-83.180	0.049
27	-85.561	-85.510	0.051
28	-102.343	-102.350	-0.007
29	-55.272	-55.300	-0.028
30	-99.403	-99.410	-0.007
31	-97.266	-97.240	0.026
32	-69.216	-69.170	0.046
33	-100.183	-100.140	0.043
34	-29.135	-29.090	0.045
35	-63.283	-63.310	-0.027
36	-83.872	-83.810	0.062
37	-101.659	-101.620	0.039
38	-40.030	-40.020	0.010
39	-75.457	-75.400	0.057
40	-101.098	-101.110	-0.012
AH8516	-91.319	-91.320	-0.001
DW0236	-52.891	-52.790	0.101
DW0037	-92.174	-92.220	-0.046
DW0236	-52.887	-	-
DW0240	-87.023	-87.020	0.003
DW1455	-89.615	-89.620	-0.005
DW9013	-91.743	-	-
DW9127	-101.385	-	-
DX0598	-92.424	-92.450	-0.026
<b>Average</b>			<b>0.005</b>
<b>Standard Deviation</b>			<b>0.036</b>
<b>RMS</b>			<b>0.036</b>

# Appendix I

## Final Coordinates and Elevations



**Dewberry and Davis**  
Salton Sea Lidar Campaign Control Survey  
**FINAL ADJUSTED COORDINATES**

Horizontal Datum: NAD83(CORS)  
Epoch: 2010.73  
Linear Unit: International Meter

Point	Latitude				Longitude				Ellipsoid Height	Standard Deviation			Description
	°	'	''	mm	°	'	''	mm		ρ	λ	h	
<b>Base Stations</b>													
TRM	N	33	38	10.48749	W	116	09	43.52624	-68.824	0.002	0.002	0.011	PK Nail set at Jackie Cochrane Regional Airport
<b>Lidar Check Points</b>													
1	N	33	32	23.97266	W	116	06	42.26193	-93.211	0.006	0.005	0.012	Natural ground - dirt
2	N	33	32	23.03572	W	116	01	03.94788	-89.147	0.009	0.006	0.019	Natural ground - dirt
3	N	33	34	23.65651	W	115	59	56.86101	-11.306	0.006	0.006	0.018	Surface of gravel road
4	N	33	31	06.06936	W	115	56	12.26312	-101.778	0.007	0.006	0.016	Top of concrete slab
5	N	33	29	29.81093	W	115	51	46.99338	-28.309	0.006	0.006	0.012	Surface of dirt road
6	N	33	26	54.47667	W	115	50	46.19816	-96.612	0.006	0.005	0.012	Surface of gravel road
7	N	33	28	19.87098	W	115	49	58.92353	-75.114	0.006	0.005	0.011	Surface of dirt road
8	N	33	25	16.94213	W	115	50	02.97915	-101.964	0.005	0.005	0.014	Surface of gravel beach
9	N	33	26	37.15462	W	115	47	24.82921	-66.935	0.007	0.005	0.015	Natural ground - dirt
10	N	33	24	12.60207	W	115	46	11.63621	-42.754	0.006	0.005	0.013	Surface of gravel road
11	N	33	23	53.62341	W	115	42	55.18540	-83.212	0.005	0.004	0.009	Surface of mud flats
12	N	33	22	26.85875	W	115	42	35.58743	-94.809	0.004	0.004	0.009	Natural ground - dirt
13	N	33	20	55.17375	W	115	43	58.18988	-100.785	0.006	0.005	0.013	Surface of gravel ramp
14	N	33	22	49.73682	W	115	38	35.27062	-49.797	0.005	0.004	0.013	Natural ground - gravel
15	N	33	21	35.45311	W	115	38	31.04337	-88.365	0.005	0.004	0.013	Natural ground - dirt
16	N	33	18	33.09806	W	115	33	22.77639	-52.238	0.006	0.004	0.015	Surface of concrete bridge
17	N	33	15	48.22133	W	115	35	09.71019	-99.210	0.005	0.005	0.010	Surface of gravel parking lot
18	N	33	15	13.66409	W	115	32	14.88474	-82.996	0.003	0.003	0.007	Surface of gravel road
19	N	33	12	19.41530	W	115	31	39.82595	-90.565	0.006	0.005	0.013	Top of dirt levee
20	N	33	09	43.64164	W	115	32	51.21188	-95.688	0.007	0.005	0.014	Top of dirt levee
21	N	33	10	34.51182	W	115	37	21.21669	-104.036	0.003	0.003	0.009	Surface of mud flats
22	N	33	08	25.49926	W	115	36	52.18724	-98.109	0.005	0.004	0.014	Top of concrete slab
23	N	33	04	29.11165	W	115	39	27.02115	-92.739	0.004	0.004	0.009	Top of dirt levee
24	N	33	06	35.01014	W	115	41	15.46325	-102.576	0.006	0.005	0.014	Top of dirt levee
25	N	33	02	30.17927	W	115	42	48.99837	-81.786	0.008	0.006	0.015	Asphalt road surface
26	N	33	04	51.87352	W	115	45	09.71434	-83.227	0.007	0.005	0.013	Asphalt road surface
27	N	33	06	33.26671	W	115	50	25.67131	-85.560	0.007	0.005	0.018	Natural ground - dirt
28	N	33	08	21.21067	W	115	47	31.22944	-102.341	0.008	0.006	0.021	Dirt road surface
29	N	33	09	43.50475	W	115	52	17.07392	-55.271	0.009	0.006	0.019	Asphalt road surface
30	N	33	11	32.97313	W	115	50	20.25442	-99.401	0.007	0.007	0.016	Top of dirt levee
31	N	33	14	36.80923	W	115	52	45.90361	-97.265	0.006	0.006	0.012	Surface of mud flats
32	N	33	13	31.06526	W	115	54	48.98425	-69.215	0.008	0.005	0.018	Natural ground - dirt
33	N	33	17	58.53741	W	115	55	04.04633	-100.182	0.004	0.004	0.013	Asphalt road extension
34	N	33	16	29.82380	W	115	58	52.69035	-29.134	0.003	0.003	0.008	Natural ground - dirt
35	N	33	20	58.37632	W	116	01	05.70280	-63.282	0.006	0.004	0.011	Natural ground - dirt
36	N	33	24	19.21937	W	116	02	43.53935	-83.871	0.007	0.006	0.014	Surface of gravel parking lot
37	N	33	27	45.77549	W	116	03	41.07415	-101.659	0.008	0.006	0.018	Surface of gravel road
38	N	33	26	25.67922	W	116	05	43.49831	-40.029	0.007	0.005	0.013	Natural ground - dirt
39	N	33	28	51.62022	W	116	06	45.31248	-75.456	0.015	0.013	0.040	Top of concrete slab
40	N	33	29	55.70436	W	116	04	46.14116	-101.098	0.007	0.006	0.019	Surface of dirt road
<b>Existing NGS Benchmarks - Adjusted Coordinates and Elevations</b>													
AH8516	N	33	23	39.15419	W	115	47	47.28011	-91.369	0.006	0.005	0.016	SS rod in sleeve - 5cm below ground
DW0037	N	33	22	17.02156	W	115	40	36.90233	-92.093	0.006	0.005	0.015	BM disk in concrete monument - 8cm above ground
DW0236	N	33	19	11.77312	W	115	59	38.41592	-52.887	0.004	0.003	0.007	Steel rod without sleeve - flush with sloping ground
DW0240	N	33	07	49.56364	W	115	51	24.75306	-86.921	0.009	0.006	0.024	BM disk in concrete monument - 10cm above ground



Point	Latitude				Longitude				Ellipsoid Height	Standard Deviation			Description
	°	'	''	'''	°	'	''	'''		ρ	λ	h	
DX0598	N	33	33	53.31834	W	116	04	23.54905	-92.464	0.007	0.006	0.019	Steel rod without sleeve - 4cm below ground
<b>CGPS Stations</b>													
GLRS	N	33	16	29.31042	W	115	31	16.89020	-47.867	-	-	-	Antenna = ASH701945C_M
P489	N	33	17	46.35313	W	116	06	41.74107	291.085	0.001	0.001	0.006	Antenna = TRM29659.00
P491	N	33	34	28.83021	W	116	13	36.51934	5.023	-	-	-	Antenna = TRM29659.00
P495	N	33	02	41.84441	W	115	37	42.16617	-83.213	0.002	0.002	0.007	Antenna = TRM29659.00
P504	N	33	30	59.06379	W	115	45	57.00099	84.804	-	-	-	Antenna = TRM29659.00
P505	N	33	25	25.93184	W	115	41	13.14995	-57.019	-	-	-	Antenna = TRM29659.00
P507	N	33	11	59.90190	W	115	36	44.60941	-77.652	-	-	-	Antenna = TRM29659.00
P508	N	33	14	51.99617	W	115	25	43.29015	11.480	0.002	0.002	0.008	Antenna = TRM29659.00
SLMS	N	33	17	32.00638	W	115	58	40.18325	-45.158	-	-	-	Antenna = ASH701945C_M
THMG	N	33	39	02.29054	W	116	04	38.05130	34.417	-	-	-	Antenna = TRM41249.00

**NOTES:**

- Ellipsoid heights of the CORS are to the antenna reference point (ARP)
- Shaded records indicate constrained values take from McGee Survey



**Dewberry and Davis**  
Salton Sea Lidar Campaign Control Survey  
**FINAL ADJUSTED COORDINATES**

Horizontal Datum: NAD83(CORS)  
Epoch: 2010.78  
Projection: UTM Zone 11  
Vertical Datum: NAVD88  
Geoid Model: GEOID09  
Linear Unit: International Meter

Point	Northing (N)	Easting (E)	Elevation (H)	Standard Deviation			Description
				N	E	H	
<b>Base Stations</b>							
TRM	3722139.664	577708.458	-35.506	0.002	0.002	0.011	PK Nail set at Jackie Cochrane Regional Airport
<b>Lidar Check Points</b>							
1	3711506.378	582469.754	-59.777	0.006	0.005	0.012	Natural ground - dirt
2	3711556.222	591195.475	-55.584	0.009	0.006	0.019	Natural ground - dirt
3	3715287.776	592889.852	22.080	0.006	0.006	0.018	Surface of gravel road
4	3709259.925	598742.710	-68.264	0.007	0.006	0.016	Top of concrete slab
5	3706367.793	605618.596	5.156	0.006	0.006	0.012	Surface of dirt road
6	3701600.921	607240.619	-62.973	0.006	0.005	0.012	Surface of gravel road
7	3704244.631	608431.658	-41.600	0.006	0.005	0.011	Surface of dirt road
8	3698609.391	608390.169	-68.249	0.005	0.005	0.014	Surface of gravel beach
9	3701126.529	612445.963	-33.348	0.007	0.005	0.015	Natural ground - dirt
10	3696696.579	614388.502	-9.058	0.006	0.005	0.013	Surface of gravel road
11	3696173.368	619470.544	-49.573	0.005	0.004	0.009	Surface of mud flats
12	3693507.324	620009.960	-61.093	0.004	0.004	0.009	Natural ground - dirt
13	3690657.285	617909.752	-66.986	0.006	0.005	0.013	Surface of gravel ramp
14	3694290.890	626210.929	-16.228	0.005	0.004	0.013	Natural ground - gravel
15	3692004.394	626349.994	-54.691	0.005	0.004	0.013	Natural ground - dirt
16	3686494.996	634395.270	-18.448	0.006	0.004	0.015	Surface of concrete bridge
17	3681378.971	631698.629	-65.292	0.005	0.005	0.010	Surface of gravel parking lot
18	3680376.910	636237.095	-49.069	0.003	0.003	0.007	Surface of gravel road
19	3675022.844	637219.925	-56.547	0.006	0.005	0.013	Top of dirt levee
20	3670199.271	635438.185	-61.583	0.007	0.005	0.014	Top of dirt levee
21	3671671.514	628423.239	-69.949	0.003	0.003	0.009	Surface of mud flats
22	3667707.991	629227.671	-63.934	0.005	0.004	0.014	Top of concrete slab
23	3660375.399	625309.019	-58.406	0.004	0.004	0.009	Top of dirt levee
24	3664217.289	622448.640	-68.294	0.006	0.005	0.014	Top of dirt levee
25	3656646.947	620116.674	-47.417	0.008	0.006	0.015	Asphalt road surface
26	3660966.800	616414.778	-48.909	0.007	0.005	0.013	Asphalt road surface
27	3663995.529	608188.319	-51.334	0.007	0.005	0.018	Natural ground - dirt
28	3667371.006	612671.382	-68.119	0.008	0.006	0.021	Dirt road surface
29	3669822.899	605237.792	-21.150	0.009	0.006	0.019	Asphalt road surface



Point	Northing (N)	Easting (E)	Elevation (H)	Standard Deviation			Description
				N	E	H	
30	3673227.374	608226.422	-65.288	0.007	0.007	0.016	Top of dirt levee
31	3678848.028	604394.251	-63.248	0.006	0.006	0.012	Surface of mud flats
32	3676789.620	601230.061	-35.235	0.008	0.005	0.018	Natural ground - dirt
33	3685023.178	600754.837	-66.260	0.004	0.004	0.013	Asphalt road extension
34	3682231.462	594868.188	4.664	0.003	0.003	0.008	Natural ground - dirt
35	3690469.335	591349.363	-29.654	0.006	0.004	0.011	Natural ground - dirt
36	3696631.414	588763.831	-50.374	0.007	0.006	0.014	Surface of gravel parking lot
37	3702979.464	587220.230	-68.146	0.008	0.006	0.018	Surface of gravel road
38	3700484.610	584081.459	-6.760	0.007	0.005	0.013	Natural ground - dirt
39	3704965.577	582447.006	-42.153	0.015	0.013	0.040	Top of concrete slab
40	3706966.042	585505.128	-67.595	0.007	0.006	0.019	Surface of dirt road
<b>Existing NGS Benchmarks - Adjusted Coordinates and Elevations</b>							
AH8516	3695637.522	611929.704	-57.623	0.006	0.005	0.016	SS rod in sleeve - 5cm below ground
DW0037	3693242.824	623080.804	-58.412	0.006	0.005	0.015	BM disk in concrete monument - 8cm above ground
DW0236	3687207.684	593637.200	-19.147	0.004	0.003	0.007	Steel rod without sleeve - flush with sloping ground
DW0240	3666328.477	606631.364	-52.735	0.009	0.006	0.024	BM disk in concrete monument - 10cm above ground
DX0598	3714289.429	586022.679	-58.962	0.007	0.006	0.019	Steel rod without sleeve - 4cm below ground
<b>CGPS Stations</b>							
GLRS	3682727.934	637704.872	-13.990	0.001	0.001	0.006	Antenna = ASH701945C_M
P489	3684477.557	582714.023	324.370	0.001	0.001	0.006	Antenna = TRM29659.00
P491	3715266.192	571757.088	37.863	0.002	0.002	0.007	Antenna = TRM29659.00
P495	3657106.893	628071.050	-48.840	0.002	0.002	0.007	Antenna = TRM29659.00
P504	3709219.903	614617.865	117.885	0.001	0.001	0.006	Antenna = TRM29659.00
P505	3699049.341	622070.669	-23.572	0.001	0.001	0.006	Antenna = TRM29659.00
P507	3674313.969	629336.502	-43.614	0.002	0.001	0.006	Antenna = TRM29659.00
P508	3679856.682	646380.795	45.353	0.002	0.002	0.008	Antenna = TRM29659.00
SLMS	3684149.716	595172.993	-11.355	0.001	0.001	0.006	Antenna = ASH701945C_M
THMG	3723802.137	585563.925	67.573	0.002	0.001	0.006	Antenna = TRM41249.00

**Appendix II**  
**Fully Constrained**  
**Network Adjustment**  
Horizontal Datum: NAD83 (CORS), 2010.73  
Vertical Datum: NAVD88



```
=====
Salton Sea; NAD83(CORS96); NAVD88 via AH8516
Microsearch GeoLab, V2001.9.20.0          GRS 80          UNITS: m,DMS  Page 0001
=====
```

Tue Nov 30 13:39:55 2010

Input file: \\tsclient\C\projects 2010\Dewberry\Salton Sea\Geolab\Salton\_primary\_c2.iob  
Output file: \\tsclient\C\projects 2010\Dewberry\Salton Sea\Geolab\Salton\_primary\_c2.lst  
Options file: C:\Program Files\Microsearch\GeoLab\default.gpj

Geoid File: c:\ngs\geoid09\g2009u05pc.gsp

PARAMETERS		OBSERVATIONS	
Description	Number	Description	Number
No. of Stations	11	Directions	0
Coord Parameters	33	Distances	0
Free Latitudes	11	Azimuths	0
Free Longitudes	11	Vertical Angles	0
Free Heights	11	Zenithal Angles	0
Fixed Coordinates	0	Angles	0
Astro. Latitudes	0	Heights	7
Astro. Longitudes	0	Height Differences	0
Geoid Records	0	Auxiliary Params.	0
All Aux. Pars.	0	2-D Coords.	14
Direction Pars.	0	2-D Coord. Diffs.	0
Scale Parameters	0	3-D Coords.	0
Constant Pars.	0	3-D Coord. Diffs.	57
Rotation Pars.	0		
Translation Pars.	0		
	-----		-----
Total Parameters	33	Total Observations	78
Degrees of Freedom =		45	

SUMMARY OF SELECTED OPTIONS

OPTION	SELECTION
Computation Mode	Adjustment
Maximum Iterations	5
Convergence Criterion	0.00100
Residual Rejection Criterion	Tau Max
Confidence Region Types	1D 2D Station Relative
Relative Confidence Regions	Connected Only
Variance Factor (VF) Known	Yes
Scale Covariance Matrix With VF	Yes
Scale Residual Variances With VF	No
Force Convergence in Max Iters	No
Distances Contribute To Heights	No
Compute Full Inverse	Yes



```
=====
                        Salton Sea; NAD83(CORS96); NAVD88 via AH8516
Microsearch GeoLab, V2001.9.20.0          GRS 80          UNITS: m,DMS  Page 0002
=====
Optimize Band Width          | Yes
Generate Initial Coordinates | Yes
Re-Transform Obs After 1st Pass | Yes
Geoid Interpolation Method   | Bi-Quadratic
-----
```



=====

Salton Sea; NAD83(CORS96); NAVD88 via AH8516  
Microsearch GeoLab, V2001.9.20.0 GRS 80 UNITS: m,DMS Page 0003

=====

Adjusted NEO Coordinates:

CODE	FFF	STATION	NORTHING STD DEV	EASTING STD DEV	O-HEIGHT STD DEV	MAPPROJ	
NEO	000	GLRS	3706805.274 0.001	1197241.047 0.001	-13.990 0.006	UTM 10	m 0
SFMC		GLRS	1.0055994040	1.0000021972	4 7 11.190000	UTM 10	
NEO	000	P489	3705371.589 0.001	1141944.723 0.001	324.370 0.006	UTM 10	m 0
SFMC		P489	1.0046847700	0.9999490606	3 47 40.060000	UTM 10	
NEO	000	P491	3735622.182 0.002	1129161.388 0.002	37.863 0.007	UTM 10	m 0
SFMC		P491	1.0044838226	0.9999940537	3 45 28.980000	UTM 10	
NEO	000	P495	3680523.161 0.002	1189050.601 0.002	-48.839 0.007	UTM 10	m 0
SFMC		P495	1.0054594407	1.0000076702	4 2 8.110000	UTM 10	
NEO	000	P504	3732056.983 0.001	1172521.872 0.001	117.886 0.006	UTM 10	m 0
SFMC		P504	1.0051808837	0.9999814865	4 0 34.360000	UTM 10	
NEO	000	P505	3722282.447 0.001	1180595.861 0.001	-23.572 0.006	UTM 10	m 0
SFMC		P505	1.0053159305	1.0000037019	4 2 37.400000	UTM 10	
NEO	000	P507	3697872.140 0.002	1189326.686 0.001	-43.615 0.006	UTM 10	m 0
SFMC		P507	1.0054639454	1.0000068497	4 3 40.160000	UTM 10	
NEO	000	P508	3704425.571 0.002	1206119.621 0.002	45.352 0.008	UTM 10	m 0
SFMC		P508	1.0057533570	0.9999928776	4 10 5.720000	UTM 10	
NEO	000	SLMS	3705764.980 0.001	1154465.248 0.001	-11.354 0.006	UTM 10	m 0
SFMC		SLMS	1.0048852272	1.0000017832	3 52 5.720000	UTM 10	
NEO	000	THMG	3744992.490 0.002	1142513.692 0.001	67.573 0.006	UTM 10	m 0
SFMC		THMG	1.0046934033	0.9999893878	3 50 57.300000	UTM 10	
NEO	000	TRM	3742865.094 0.002	1134729.968 0.002	-35.506 0.011	UTM 10	m 0
SFMC		TRM	1.0045706599	1.0000055763	3 48 1.160000	UTM 10	



=====  
 Salton Sea; NAD83(CORS96); NAVD88 via AH8516  
 Microsearch GeoLab, V2001.9.20.0                      GRS 80                      UNITS: m,DMS    Page 0004  
 =====

Adjusted PLH Coordinates:

CODE	FFF	STATION	LATITUDE		LONGITUDE		ELIP-HEIGHT		
			STD	DEV	STD	DEV	STD	DEV	
PLH	000	GLRS	N 33 16	29.31035	W115 31	16.89028	-47.865	m	0
				0.001		0.001	0.006		
PLH	000	P489	N 33 17	46.35313	W116 6	41.74107	291.085	m	0
				0.001		0.001	0.006		
PLH	000	P491	N 33 34	28.83033	W116 13	36.51915	5.022	m	0
				0.002		0.002	0.007		
PLH	000	P495	N 33 2	41.84441	W115 37	42.16617	-83.213	m	0
				0.002		0.002	0.007		
PLH	000	P504	N 33 30	59.06374	W115 45	57.00098	84.797	m	0
				0.001		0.001	0.006		
PLH	000	P505	N 33 25	25.93186	W115 41	13.15016	-57.014	m	0
				0.001		0.001	0.006		
PLH	000	P507	N 33 11	59.90190	W115 36	44.60942	-77.646	m	0
				0.002		0.001	0.006		
PLH	000	P508	N 33 14	51.99617	W115 25	43.29015	11.480	m	0
				0.002		0.002	0.008		
PLH	000	SLMS	N 33 17	32.00647	W115 58	40.18315	-45.153	m	0
				0.001		0.001	0.006		
PLH	000	THMG	N 33 39	2.29043	W116 4	38.05124	34.406	m	0
				0.002		0.001	0.006		
PLH	000	TRM	N 33 38	10.48749	W116 9	43.52624	-68.824	m	0
				0.002		0.002	0.011		

```

=====
                        Salton Sea; NAD83(CORS96); NAVD88 via AH8516
Microsearch GeoLab, V2001.9.20.0          GRS 80          UNITS: m,DMS  Page 0005
=====

```

Geoid Values:

CODE	STATION	N/S DEFLECTION			E/W DEFLECTION			UNDULATION
-----								
GEOI	GLRS	- 0 0	4.70	- 0 0	0.98		-33.875 m	
GEOI	P489	- 0 0	7.22	0 0	8.60		-33.285 m	
GEOI	P491	0 0	8.55	0 0	17.85		-32.841 m	
GEOI	P495	- 0 0	2.70	- 0 0	0.38		-34.373 m	
GEOI	P504	- 0 0	13.81	- 0 0	4.43		-33.088 m	
GEOI	P505	- 0 0	10.41	- 0 0	6.89		-33.442 m	
GEOI	P507	- 0 0	3.69	- 0 0	0.81		-34.032 m	
GEOI	P508	- 0 0	5.03	- 0 0	3.06		-33.872 m	
GEOI	SLMS	- 0 0	0.72	0 0	6.05		-33.799 m	
GEOI	THMG	- 0 0	9.51	- 0 0	7.37		-33.167 m	
GEOI	TRM	- 0 0	0.55	0 0	3.34		-33.318 m	

```
=====
                        Salton Sea; NAD83(CORS96); NAVD88 via AH8516
Microsearch GeoLab, V2001.9.20.0          GRS 80          UNITS: m,DMS  Page 0006
=====
```

Residuals (critical value = 3.403):

NOTE: Observation values shown are reduced to mark-to-mark.

TYPE	AT	FROM	TO	OBSERVATION STD DEV	RESIDUAL STD DEV	STD RES PPM
ELAT	P507			N 33 11 59.90190 0.003	0.000 0.002	0.024
ELON	P507			W115 36 44.60941 0.003	-0.000 -0.000	-0.000
ELAT	THMG			N 33 39 2.29054 0.003	-0.003 0.002	-1.394
ELON	THMG			W116 04 38.05130 0.003	0.001 -0.000	0.001
ELAT	SLMS			N 33 17 32.00638 0.003	0.003 -0.000	0.003
ELON	SLMS			W115 58 40.18320 0.003	0.001 -0.000	0.001
ELAT	P505			N 33 25 25.93184 0.003	0.001 -0.000	0.001
ELON	P505			W115 41 13.14995 0.003	-0.005 -0.000	-0.005
ELAT	P491			N 33 34 28.83021 0.003	0.004 0.002	1.566
ELON	P491			W116 13 36.51934 0.003	0.005 -0.000	0.005
ELAT	P504			N 33 30 59.06379 0.003	-0.002 -0.000	-0.002
ELON	P504			W115 45 57.00099 0.003	0.000 -0.000	0.000
ELAT	GLRS			N 33 16 29.31042 0.003	-0.002 -0.000	-0.002
ELON	GLRS			W115 31 16.89020 0.003	-0.002 -0.000	-0.002
EHGT	GLRS			-47.86700 0.010	0.002 0.008	0.189
EHGT	P491			5.02300 0.010	-0.001 0.007	-0.128
EHGT	P504			84.80400 0.010	-0.007 0.008	-0.813
EHGT	P507			-77.65200 0.010	0.006 0.008	0.722
EHGT	SLMS			-45.15800 0.010	0.005 0.008	0.642
EHGT	THMG			34.41700 0.010	-0.011 0.008	-1.352
EHGT	P505			-57.01900 0.010	0.005 0.008	0.639
GROUP: 00000, Salton_primary.asc						
DXCT		THMG	P491	-14504.73300 0.004	0.000 0.003	0.042 0.01
DYCT		THMG	P491	1953.44500	0.001	0.236



=====

Salton Sea; NAD83(CORS96); NAVD88 via AH8516  
Microsearch GeoLab, V2001.9.20.0 GRS 80 UNITS: m,DMS Page 0007

=====

Residuals (critical value = 3.403):

NOTE: Observation values shown are reduced to mark-to-mark.

TYPE	AT	FROM	TO	OBSERVATION STD DEV	RESIDUAL STD DEV	STD RES PPM
				0.007	0.006	0.08
DZCT		THMG	P491	-7032.83500	-0.001	-0.334
				0.006	0.004	0.08
GROUP: 00001, Salton_primary.asc						
DXCT		THMG	P504	22381.95400	0.004	1.224
				0.004	0.003	0.12
DYCT		THMG	P504	-20081.79400	0.003	0.482
				0.008	0.006	0.09
DZCT		THMG	P504	-12375.19100	-0.003	-0.658
				0.006	0.005	0.10
GROUP: 00002, Salton_primary.asc						
DXCT		SLMS	P489	-11211.08100	-0.003	-1.029
				0.004	0.003	0.22
DYCT		SLMS	P489	5436.09000	-0.003	-0.591
				0.007	0.005	0.24
DZCT		SLMS	P489	554.02700	0.002	0.497
				0.005	0.004	0.15
GROUP: 00004, Salton_primary.asc						
DXCT		GLRS	P507	-9606.15000	-0.002	-0.576
				0.004	0.003	0.13
DYCT		GLRS	P507	-419.73900	0.000	0.098
				0.007	0.005	0.04
DZCT		GLRS	P507	-6958.36800	-0.002	-0.434
				0.005	0.004	0.13
GROUP: 00005, Salton_primary.asc						
DXCT		P508	P495	-22077.90000	0.001	0.376
				0.004	0.003	0.04
DYCT		P508	P495	-2997.95800	-0.001	-0.135
				0.008	0.006	0.03
DZCT		P508	P495	-18885.49300	-0.001	-0.292
				0.006	0.005	0.05
GROUP: 00006, Salton_primary.asc						
DXCT		P508	P504	-21235.50100	0.001	0.238
				0.004	0.003	0.02
DYCT		P508	P504	28282.60500	-0.004	-0.673
				0.008	0.006	0.10
DZCT		P508	P504	24919.15600	0.001	0.307
				0.006	0.005	0.03
GROUP: 00007, Salton_primary.asc						
DXCT		GLRS	P495	-15011.62300	0.000	0.001
				0.004	0.003	0.00
DYCT		GLRS	P495	-8240.98200	-0.001	-0.170
				0.008	0.007	0.04
DZCT		GLRS	P495	-21359.85600	0.002	0.447
				0.006	0.005	0.08
GROUP: 00008, Salton_primary.asc						

=====

Salton Sea; NAD83(CORS96); NAVD88 via AH8516  
Microsearch GeoLab, V2001.9.20.0 GRS 80 UNITS: m,DMS Page 0008

=====

Residuals (critical value = 3.403):

NOTE: Observation values shown are reduced to mark-to-mark.

TYPE AT	FROM	TO	OBSERVATION STD DEV	RESIDUAL STD DEV	STD RES PPM
DXCT	P489	P491	-2005.41500 0.004	-0.001 0.003	-0.431 0.05
DYCT	P489	P491	20213.16500 0.008	-0.003 0.006	-0.464 0.09
DZCT	P489	P491	25616.93500 0.006	0.003 0.005	0.545 0.08
GROUP: 00009, Salton_primary.asc					
DXCT	P489	P495	34038.87500 0.005	0.001 0.003	0.266 0.02
DYCT	P489	P495	-33102.64300 0.009	0.008 0.007	1.202 0.15
DZCT	P489	P495	-23530.06900 0.006	-0.003 0.005	-0.589 0.05
GROUP: 00010, Salton_primary.asc					
DXCT	SLMS	P507	28233.26200 0.004	0.002 0.003	0.511 0.05
DYCT	SLMS	P507	-19845.30300 0.008	-0.000 0.006	-0.045 0.01
DZCT	SLMS	P507	-8574.56000 0.006	0.001 0.005	0.252 0.03
GROUP: 00011, Salton_primary.asc					
DXCT	P504	P489	-34881.27700 0.005	0.003 0.004	0.699 0.06
DYCT	P504	P489	1822.07200 0.009	0.003 0.007	0.467 0.08
DZCT	P504	P489	-20274.57900 0.006	-0.001 0.005	-0.175 0.02
GROUP: 00013, Salton_primary.asc					
DXCT	P495	P507	5405.46900 0.004	0.002 0.003	0.844 0.14
DYCT	P495	P507	7821.24100 0.008	0.004 0.006	0.627 0.21
DZCT	P495	P507	14401.48600 0.006	-0.002 0.004	-0.420 0.10
GROUP: 00014, Salton_primary.asc					
DXCT	GLRS	P508	7066.27500 0.003	0.001 0.002	0.391 0.08
DYCT	GLRS	P508	-5243.02100 0.006	-0.003 0.004	-0.853 0.36
DZCT	GLRS	P508	-2474.36000 0.005	0.001 0.003	0.198 0.06
GROUP: 00016, Salton_primary.asc					
DXCT	TRM	THMG	7419.36700 0.005	0.001 0.003	0.391 0.16
DYCT	TRM	THMG	-2748.76500 0.010	-0.001 0.006	-0.115 0.09



```
=====
                Salton Sea; NAD83(CORS96); NAVD88 via AH8516
Microsearch GeoLab, V2001.9.20.0          GRS 80          UNITS: m,DMS  Page 0009
=====
```

Residuals (critical value = 3.403):

NOTE: Observation values shown are reduced to mark-to-mark.

TYPE AT	FROM	TO	OBSERVATION STD DEV	RESIDUAL STD DEV	STD RES PPM
DZCT	TRM	THMG	1385.89800 0.008	0.003 0.005	0.523 0.32
GROUP: 00017, Salton_primary.asc					
DXCT	TRM	P491	-7085.36300 0.006	-0.002 0.004	-0.415 0.17
DYCT	TRM	P491	-795.32000 0.011	0.001 0.007	0.078 0.06
DZCT	TRM	P491	-5646.93300 0.008	-0.003 0.006	-0.486 0.30
GROUP: 00018, Salton_primary.asc					
DXCT	THMG	P489	-12499.31800 0.005	0.002 0.004	0.411 0.04
DYCT	THMG	P489	-18259.72000 0.009	0.004 0.007	0.582 0.11
DZCT	THMG	P489	-32649.77200 0.007	-0.002 0.006	-0.365 0.05
GROUP: 00000, P505.asc					
DXCT	P505	P504	-4197.06800 0.004	-0.004 0.003	-1.358 0.28
DYCT	P505	P504	8174.14800 0.007	-0.001 0.005	-0.171 0.07
DZCT	P505	P504	8639.76300 0.005	0.004 0.004	1.014 0.30
GROUP: 00001, P505.asc					
DXCT	P505	GLRS	9972.15200 0.004	0.001 0.003	0.325 0.04
DYCT	P505	GLRS	-14865.42600 0.008	-0.003 0.006	-0.594 0.15
DZCT	P505	GLRS	-13805.03100 0.006	-0.000 0.004	-0.035 0.01
GROUP: 00002, P505.asc					
DXCT	P505	SLMS	-27867.26200 0.004	-0.000 0.003	-0.062 0.01
DYCT	P505	SLMS	4560.13500 0.008	0.000 0.006	0.055 0.01
DZCT	P505	SLMS	-12188.84100 0.006	-0.001 0.005	-0.199 0.03

```
=====
Salton Sea; NAD83(CORS96); NAVD88 via AH8516
Microsearch GeoLab, V2001.9.20.0      GRS 80      UNITS: m,DMS  Page 0010
=====
```

```
-----
S T A T I S T I C S      S U M M A R Y
-----
```

Residual Critical Value Type	Tau Max
Residual Critical Value	3.4030
Number of Flagged Residuals	0
Convergence Criterion	0.0010
Final Iteration Counter Value	2
Confidence Level Used	95.0000
Estimated Variance Factor	1.0286
Number of Degrees of Freedom	45

```
-----
Chi-Square Test on the Variance Factor:
```

```
7.0761e-01 < 1.0000 < 1.6317e+00 ?
```

```
THE TEST PASSES
-----
```

```
-----
NOTE: All confidence regions were computed using the following factors:
```

Variance factor used	=	1.0286
1-D expansion factor	=	1.9600
2-D expansion factor	=	2.4477

```
Note that, for relative confidence regions, precisions are
computed from the ratio of the major semi-axis and the spatial
distance between the two stations.
-----
```

```

=====
                Salton Sea; NAD83(CORS96); NAVD88 via AH8516
Microsearch GeoLab, V2001.9.20.0          GRS 80          UNITS: m,DMS  Page 0011
=====
2-D and 1-D Station Confidence Regions (95.000 and 95.000 percent):
STATION          MAJOR SEMI-AXIS  AZ      MINOR SEMI-AXIS  VERTICAL
-----
GLRS              0.004    2          0.003            0.012
P489              0.004  179          0.003            0.013
P491              0.004    3          0.004            0.013
P495              0.004  175          0.004            0.014
P504              0.004    5          0.003            0.011
P505              0.004    5          0.003            0.012
P507              0.004    3          0.004            0.012
P508              0.004    4          0.004            0.015
SLMS              0.004    4          0.003            0.012
THMG              0.004    4          0.004            0.012
TRM               0.006    7          0.005            0.022

```



```
=====
                          Salton Sea; NAD83(CORS96); NAVD88 via AH8516
Microsearch GeoLab, V2001.9.20.0          GRS 80          UNITS: m,DMS  Page 0012
=====
2-D and 1-D Relative Station Confidence Regions (95.000 and 95.000 percent):
FROM          TO          MAJ-SEMI  AZ  MIN-SEMI  VERTICAL  DISTANCE  PPM
-----
GLRS          P495          0.003    2   0.002    0.013    27377.107  0.11
GLRS          P505          0.003    4   0.003    0.013    22605.391  0.14
GLRS          P507          0.003    5   0.002    0.012    11869.003  0.24
GLRS          P508          0.003    6   0.002    0.012     9140.241  0.30
P489          P491          0.003    4   0.003    0.014    32692.830  0.11
P489          P495          0.004  165  0.003    0.015    52991.450  0.07
P489          P504          0.003    2   0.003    0.013    40386.654  0.08
P489          SLMS          0.003    1   0.003    0.013    12471.824  0.25
P489          THMG          0.003    4   0.003    0.014    39441.829  0.08
P491          THMG          0.003    5   0.003    0.013    16237.734  0.19
P491          TRM           0.005    7   0.004    0.020     9095.208  0.51
P495          P507          0.003    2   0.003    0.014    17256.701  0.18
P495          P508          0.003    2   0.003    0.014    29207.589  0.11
P504          P505          0.003    6   0.002    0.012    12612.599  0.24
P504          P508          0.003    4   0.003    0.015    43264.493  0.08
P504          THMG          0.003    5   0.003    0.013    32517.315  0.10
P505          SLMS          0.003    5   0.003    0.013    30756.251  0.11
P507          SLMS          0.003    4   0.003    0.014    35559.476  0.09
THMG          TRM           0.005    8   0.004    0.020     8032.650  0.57
=====
```